ASSESSMENT OF CRITICAL LIFELINE STRUCTURES: SEISMIC RESPONSE OF CALIFORNIA EARTH DAMS USING EMPIRICAL, NUMERICAL, AND EXPERIMENTAL APPROACHES

Adda Athanasopoulos-Zekkos and Makbule Ilgac

Department of Civil and Environmental Engineering
University of California, Berkeley

Abstract

This paper focuses on assessing the vibration characteristics of Briones Dam in Northern California. First, earthquake-based Horizontal-to-Vertical Spectral Ratio (eHVSR) was estimated by dividing the horizontal records by the vertical components, and the SSR was determined by comparing crest recordings with those from the abutment. Additionally, a microtremor-based HVSR was computed based on field measurements. The fundamental frequency was estimated using three empirical methods: mHVSR (*0.7* to *1 Hz*), eHVSR (*0.9* to *1.1 Hz*), and SSR (*1.2 Hz*). The slight variations among these three methods suggest the need for further investigations that consider the geological and geotechnical conditions of the dam.

Introduction

Assessing the seismic response of dams is essential for both developing new design procedures and evaluating the performance of existing structures. A key parameter in this process is the fundamental frequency, f_0 (or period, T_0), of an earth embankment dam. This frequency is critical for seismic hazard analysis, as it is used to scale design time-histories to match the dam's vibration mode with the target spectrum, and it plays an important role in preliminary design assessments. Many past studies focus on determining the fundamental period of both existing and new dams using analytical, empirical, and numerical approaches. The simple shear beam approach, introduced by Ambraseys (1960), models different vibration modes as a function of parameters such as dam height, crest length, and average shear wave velocity of the dam material assuming truncated wedge shape, rectangular canyon, and elastic layers. Subsequent improvements to this approach have been achieved through further analytical assessments. Gazetas (1987) refined the shear beam models to account for material inhomogeneity, non-rectangular canyon shapes, and nonlinear inelastic behavior. These analytical models are also cross-validated with landmark case histories. For example, Abdel-Ghaffar and Scott (1979a, b) compared one-dimensional and two-dimensional shear beam models with full-scale vibration test results and earthquake recordings. Advanced numerical techniques, such as the finite element method (FEM), effectively address all key objectives regarding seismic assessment of earth dams, including stability, displacements, and dynamic response. Over time, significant advancements in FEM capabilities have enhanced the study of the seismic behavior of dams. Initial efforts in the 1960s using finite discretization methods, laid the foundation for major developments in this area. Notably, Prevost et al. (1985), Makdisi et al. (1982), and Mejia et al. (1982, 1983) conducted two- and three-dimensional (2-D, 3-D) finite element analyses to model the complex behavior of dams under dynamic loading conditions. Today’s advanced tools enable comprehensive numerical analyses that account for three-dimensional complexities and sophisticated nonlinear coupled dynamic analysis that include

reservoir-dam hydrodynamic effects. For example, Mejia and Dawson (2008) aimed to identify the modes of vibration of Seven Oaks Dam during earthquakes and evaluate the effectiveness of 3-D and 2-D numerical models in simulating the recorded dynamic response of the dam. Pelecanos (2013) studied the effect of upstream reservoir hydrodynamic pressures on the elastic seismic response of dams. They proposed a methodology and conducted a parametric study to analyze how the reservoir influences the dam's seismic behavior. Pelecanos also examined the nonlinear seismic behavior of earth dams, using La Villita Dam in Mexico as a case study to validate their model. The results showed good agreement between the recorded and predicted data. As a result, the calibrated model was then used to further investigate the dynamic response of earth dams. Zimmaro and Ausulio (2020) performed a numerical analysis of the Farneto del Principe dam, where they tested assumptions regarding boundary conditions, degree of saturation, and the dam material properties. Their findings highlighted that soil structure interaction effects due to the flexibility of the dam foundation can produce period elongations for all modes of the dam, emphasizing the need to account for these effects in modeling.

As analytical methods become more complex, they also become more time-consuming and computationally intensive. Additionally, they require precise attention to foundation and material properties, often necessitating extensive site investigations and laboratory testing. In contrast, empirical methods offer a faster and more practical approach, providing valuable real-world insights into a dam’s performance without the need for exhaustive fieldwork. Microtremor-based measurements, in particular, are relatively inexpensive to collect, making them an efficient alternative. By combining earthquake recordings with microtremor measurements at earth dams in California, we can quickly and comprehensively analyze their seismic response, enabling rapid interpretation of dam behavior and identifying potential vulnerabilities. Building on these empirical approaches, this study focuses on the use of the microtremor- and earthquake-based data assessment method to assess the seismic behavior of dams, offering a cost-effective and efficient tool for evaluating dam performance.

The seismic response of dams is influenced by several factors, including canyon geometry, properties of dam materials, the stiffness characteristics of the foundation materials, dam-reservoir interaction, level of nonlinearity under earthquake loading, and more. These complexities make accurate seismic assessments challenging. Empirical, numerical, and analytical methods serve as the primary options to evaluate the dynamic behavior of a dam, with empirical approaches offering practical benefits due to their lower computational demands.

Empirical methods, such as the Standard Spectral Ratio (SSR) and Horizontal-to-Vertical Spectral Ratio (HVSR), are widely used to determine the fundamental frequency of a site. The SSR method, first studied by Borcherdt (1970), Lachet et al. (1996), and Haghshenas et al. (2008), compares the spectral response of seismic records at a site of interest with those from a reference site, typically on bedrock. Originally developed for free-field sites, SSR has been adapted for seismic assessments of dams, where crest recordings are compared to those from reference locations, often at the toe, downstream, or abutment, if foundation records are unavailable. This method is also known by other names in dam seismic studies, including the Crest-to-Foundation (C-F) Method and Cross Spectra Methods. In this paper, we refer to it as SSR. Previous studies utilizing this method include works by Abdel-Ghaffar and Koh (1981), Boulanger et al. (1995), Cetin et al. (2005), Hwang et al. (2008), Mejia and Dawson (2008),

Matsumoto et al. (2010), Sasaki et al. (2015), Verret and LeBoeuf (2017), Park and Kishida (2019), Correia et al. (2019), Pastén et al. (2023), and many others. These studies presented comparisons of SSR and HVSR methods using case histories to evaluate the fundamental frequency of the dams. For example, Park and Kishida (2019) analyzed the ratio of crest to foundation records of 60 dams during 54 earthquakes and investigated correlations with shaking intensities and dam geometries.

HVSR, on the other hand, is a single-station method that calculates the Fourier amplitude ratio of the horizontal to vertical components, based on the assumption that vertical components show less amplification than the horizontal ones, and that at higher frequencies. This method allows the identification of fundamental frequencies where horizontal amplification occurs at lower frequencies. Initially developed for microtremor measurements by Nogoshi and Igarashi (1971) and popularized by Nakamura (1989, 2000), HVSR was first proposed for use on earthquake recordings by Lermo and Chávez-García (1993). Although the theoretical background between the two kinds of recordings differs -and is beyond the scope of this paper-, HVSR has been applied in both ambient noise measurements (mHVSR) and earthquake recordings (eHVSR). Kawase et al. (2011, 2019) further explored the impact of various wave portions on the calculation of eHVSR and presented a comparison between mHVSR and eHVSR. Their research investigated the theoretical similarities and differences between these two methods. Studies by numerous researchers, including Field and Jacob (1995), Bonilla et al. (1997), Ktenidou et al. (2011;2016), Ghofrani et al. (2013), Zhu et al. (2020), Hassani and Atkinson (2019), Wang et al. (2023), and others have used eHVSR to evaluate the site amplification characteristics at various sites.

Both mHVSR and eHVSR have also been applied to assess the vibration characteristics of dams, as seen in studies by Oner (1984), Cetin et al. (2005), Ruiz and Pando (2011), and more recent work by Verret and LeBoeuf (2017), Correia et al. (2019), Pastén et al. (2023), Ilgac and Athanasopoulos-Zekkos (2022, 2023), Ilgac et al (2024) and Athanasopoulos-Zekkos and Ilgac (2024). These studies compared the eHVSR and mHVSR methods using case histories to evaluate the fundamental frequency of the dams. For example, Verret and LeBoeuf (2017) examined the Denis-Perron dam in Québec, Canada. The earthquake data was used to calculate the SSR, and eHVSR to estimate the different modes of vibration as well as the fundamental mode of the dam, and the results are compared with the collected ambient noise measurements (mHVSR), which indicated consistency between the frequency values obtained by different methods. In this study, we utilized both mHVSR and eHVSR methods along with the SSR method to analyze the vibration characteristics of Briones Dam. While previous studies have assessed the vibration characteristics of earth dams using analytical, empirical, and numerical approaches, systematic comparisons of empirical methods at dam sites remain limited. This study aims to address this gap by evaluating and comparing available empirical approaches, including microtremor measurements, eHVSR, and SSR, using unique case history data that was recently acquired from Briones Dam.. A field-testing program was conducted at Briones Dam in June 2024 to collect microtremor measurements at the rock abutment, dam crest, mid-dam, and dam toe. The Horizontal-to-Vertical Spectral Ratio (mHVSR and eHVSR) and Standard Spectral Ratio (SSR) approaches were employed to investigate the vibration characteristics of the Briones dam.

Description of Briones Dam

Briones Dam was built in 1964 for the primary use of water supply in Contra Costa County, San Francisco Bay area (37.9135°, -122.2092°). It is an embankment dam which was constructed over a trapezoidal valley that was established by the historic Bear Creek. The dam consists of four zones (detailed in subsequent sections) and has a maximum height of *78-m* (*256-feet*), crest width of *15.3-m* (*50-feet*), crest length of *626.7-m* (*2,056-feet*), an upstream slope of *2.8-3:1* H:V (horizontal to vertical), and a downstream slope of *2.7-2.9:1* H:V with several large benches. Instrumentation of the dam occurred in 1975 with the installation of three sensors (seismographs) at the left abutment, center, and left crest (numbered Loc1, Loc2, and Loc3). A plan view of the embankment contact with the location of the accelerometer sensors is shown in Fig. 1. The accelerometers placed at the center crest, and the one at the left crest are oriented in alignment with the dam's transverse and longitudinal directions. Due to a field change after 06/24/2014, the orientation of the sensor at the left abutment was updated from (*31°* and *121°*) to (*90°* and *360°*). Briones Dam is owned and operated by East Bay Municipal Utility District (EBMUD), and the following information is provided by personal communication with Kyle Peterson from EBMUD regarding the geology, dam material properties, and cross-section.

The dam consists of four primary zones: Zone I – III with Zone III having two differing sources. The dam was constructed by stripping native alluvial deposits out of the Bear Creek valley and excavating any weak friable bedrock to competent bedrock formations. A *2.1-m* (*7-foot*)-thick concrete cutoff wall was installed along the axis of the dam, and a grout curtain was constructed by drilling *15.2-m* (*50-foot*)-deep boreholes into the bedrock and packer grouted under pressure. The packer grouting generally showed the bedrock was relatively impervious and required very few additional grout holes with generally low grout takes and frequent grout refusal. The embankment materials were mainly sourced from Briones and Orinda formation sites near and around the embankment site to construct the dam. The formational rock materials are highly variable, featuring complex bedding, folding, weathering, and weakly cemented and predominantly composed of claystones, siltstones, and sandstones with subordinate beds of conglomerate. The embankment construction efforts primarily used lower fines content materials (such as conglomerates, sandstones, or sandy siltstones) for construction of Zone II materials, siltstones/sandy claystones for construction of Zone I, and higher fines content rock (such as claystones) for construction of Zone III that serves as the relatively impervious clay core of the dam.

Fig. 2a presents the transverse profile of Briones Dam in the upstream-downstream direction with the embankment zoning, and Fig. 2b presents the longitudinal profile along the dam axis (looking downstream) with the pre-construction topography and the stripped topography. Note that the upstream boundary underlying Zone III has a drainage blanket consisting of imported graded rock to convey seepage into a drainage blanket that discharges at the downstream toe of the dam to prevent the embankment materials from becoming saturated. The piezometric pressures in the dam are therefore low and controlled by the elevation of the drainage blanket. Table 1 summarizes the properties of dam materials along with the United Soil Classification System abbreviation, fines content, index properties, and CIUTX total stress strength parameters. Shear wave velocity measurements on the embankment material were unavailable.

The geologic unit underlying Briones Dam is primarily comprised of the Orinda formation, which serves as the bedrock. The Orinda formation is a fine grain material with a low dry unit weight, high optimum moisture, and fairly low strength parameters, and is generally sound and impervious, with the shear strength of the unfractured material having friction angle of *42 degrees* and a cohesion of *460 kPa*. The parts of the bedrock that consist of fissured or fractured material have an average friction angle of angle reported as *30 degrees* and zero cohesion (EBMUD, 1967). Fig. 3 shows that the embankment dam is situated on top of layers of various sedimentary rocks that have been folded into an anticline and subsequently eroded such that the bottom of the dam interfaces with multiple sedimentary rock layers. However, the base of the dam under the crest axis is generally dominated by claystone. Underlying the Orinda formation in the vicinity of the dam is the San Pablo Group, which is represented by a fairly thin section of lower Briones sandstone; however, the Cierbo, the Neroly, and the middle and upper sections of the San Pablo group are entirely absent there. The lower Briones section consists of massive fine-grained sandstone, and this sandstone was found in conformable contact with both the Orinda sediments, stratigraphically above, and the Rodeo shales below it (EBMUD, 1967).

Two core borings, DH-1 (37.91106°, -122.20387°) and DH-2 (37.91085°, -122.20474°), were drilled in 2015 to identify the geological conditions in the left bedrock abutment of Briones Dam to characterize the rock for seismic analyses of the outlet tower; these two borings are shown on Fig. 1 for proximity reference to the bedrock accelerometer (Loc1). The shear and compression wave velocity of the rock was measured using OYO suspension logging techniques (TERRA, 2016). Based on the two boreholes drilled at the left abutment, it was observed that extensive claystone, sandstone, and conglomerate bedding exists in the area which confirms construction data showing the dam is situated over highly complex bedding and folding (see Fig. 3). Shear wave velocity and compression wave velocity profiles at DH-1 and DH-2 are presented in Fig. 4a and the shear wave velocity classified by bedrock-type is presented in Fig 4b. A linear regression line was fit to the shear wave velocity measurements within the claystone materials; this was done to obtain a lower-bound estimate of the shear wave velocity in the upper 30 meters (V_{S30}) for the claystone bedrock formation that was considered the dominant bedrock type for seismic analysis of the outlet tower (located near the upstream toe of the dam). From this fit, the lower-bound V_{S30} was estimated as 525 m/s, as shown in Fig. 4b. An estimate of the time-averaged V_{S30} from the shear wave velocity measurements when accounting for all bedrock formation types is approximately 587 m/s. It should be noted that the shear wave velocity measurements were collected at a free-field rock outcrop (i.e., no effects of overburden) and consequently the V_{S30} of the bedrock under the axis of the embankment may be higher when accounting for the confining stress caused by the embankment over the bedrock. Rock core samples were also retrieved from DH-1 and DH-2, and unconfined compression testing was performed. As reported by TERRA (2016), the test results showed that the rocks are generally soft rock with unconfined compressive strength ranging between *1240 to 5000* kPa. However, there are occasional zones of moderately soft rocks (*5000 – 14210 kPa*) and very soft rocks (the borderline between soil and rock) that were observed

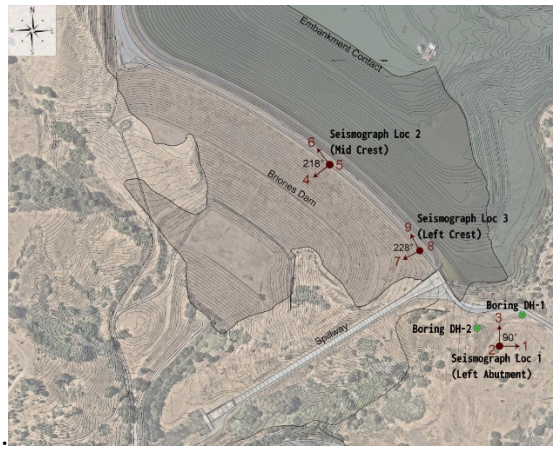

Fig. 1. Plan View of Briones Dam with CGS CSMIP Station CE 58183 Locations (Loc 1: 37.9107967,-122.2054301)

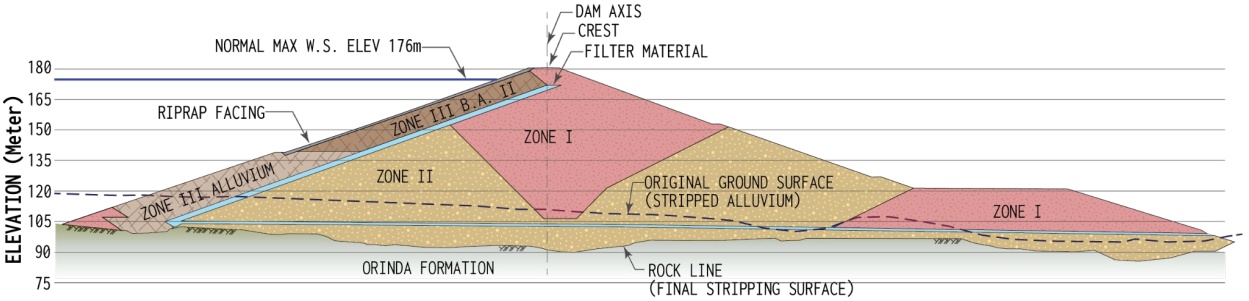

Fig. 2a. Transverse profile of Briones Dam at the maximum section (Station 15+50) in the upstream-downstream direction (1:1 scale).

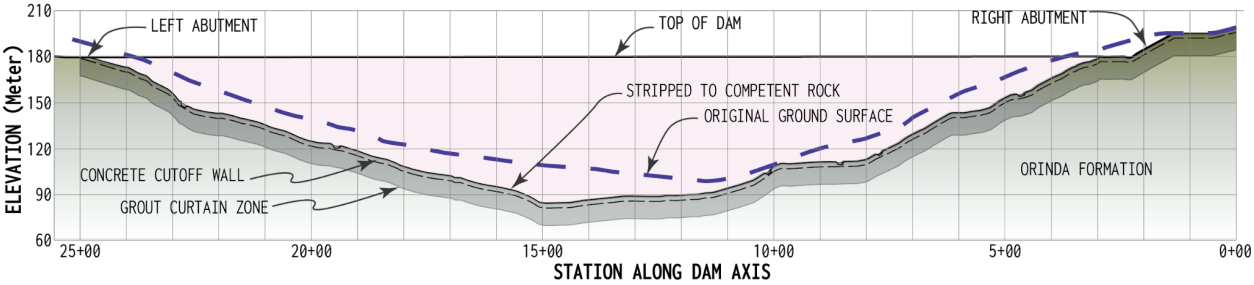

Fig. 2b. Longitudinal profile of Briones Dam along the dam axis (1:1 scale, looking downstream)

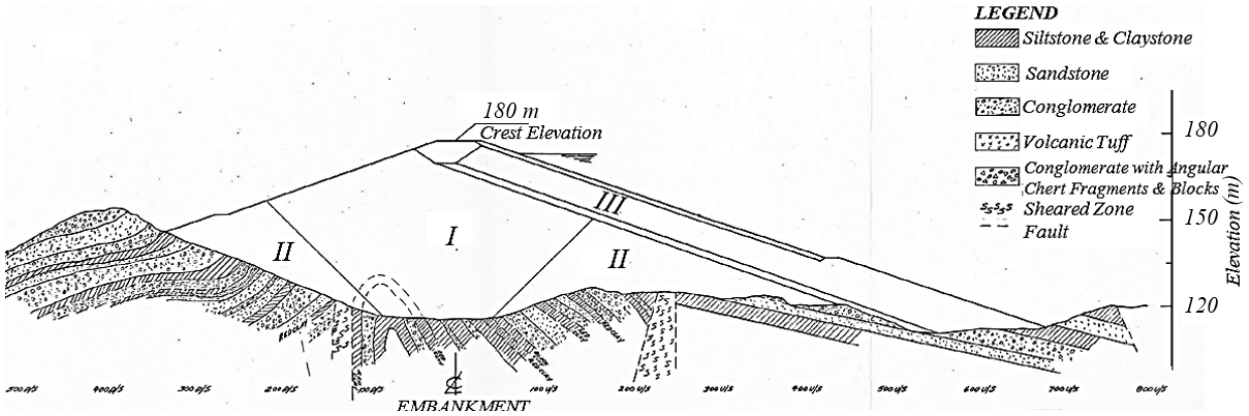

Fig. 3. Highly-interbedded and folded geology underlying Briones Dam (section at Station 8+00).

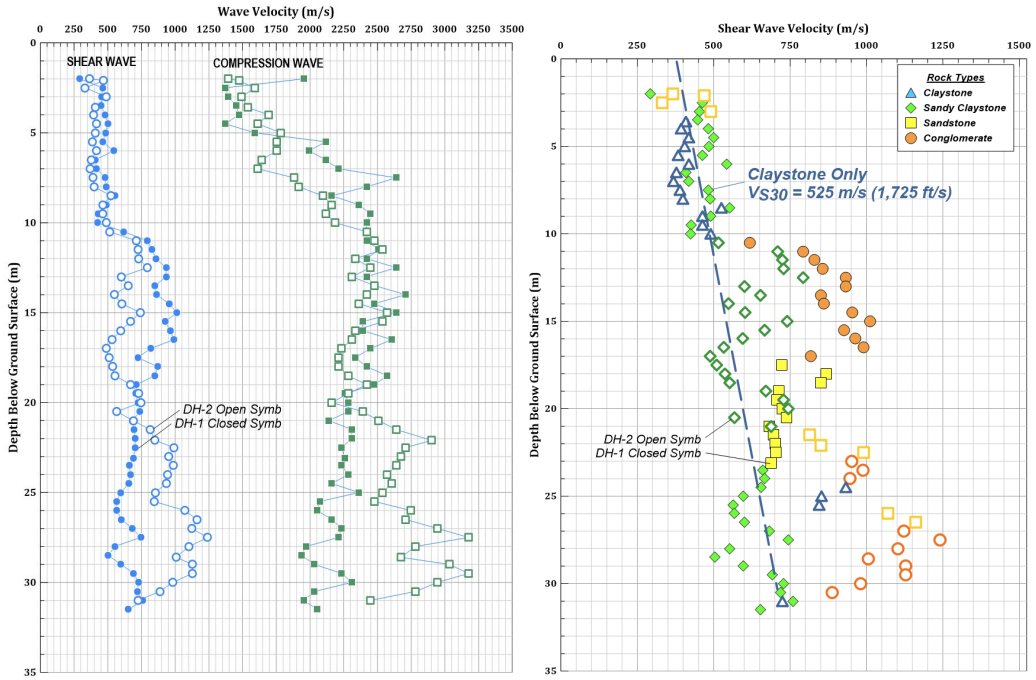

Fig. 4(a). Shear and compression wave velocity profiles at bedrock sites on the left-abutment, DH-1 and DH-2, (b). Shear wave velocity profiles at DH-1 and DH-2 classified by rock type

Table 1. Properties of the Dam Material (EBMUD, 1967)

Zone	Source	USCS	Fines Content (%)[2]	Index Properties (LL, PI)[2]	Strength Properties[1,2]
I	Six sites (abutments, reservoir basin, and hillside areas) and predominantly siltstone/claystone from Orinda Formation	CL, SC with occasional CH/MH	49±13	36±8, 17±7	$\phi = 23.1 \pm 4°$ c = 57.5±19.2 kPa

II	Silty/clayey sandstone from Briones Formation	CL, SC, SM	40±13	34±5, 12±7	ϕ = 27.6±3° c = 47.9±38.3 kPa
III (B.A. II)	Silty claystone from Orinda Formation	CL	70±6	37±4, 21±4	N/A
III (Alluvium)	Alluvium from embankment excavation	CL, CH	72±4	44±3, 25±4	ϕ = 12.6±1° c = 67±19.2 kPa

[1] Total Stress Properties from CIUTX Testing from samples collected during embankment construction.
[2] Values are mean average with one standard deviation from laboratory testing performed on samples collected during embankment construction.

Ground Motions

Briones Dam is located in the seismically active San Francisco Bay Area, near three major strike-slip fault systems: Hayward-Rodgers Creek, San Andreas, and Concord-Green Valley faults. Specifically, it lies within the East Bay Hills block, a northwest-southeast trending, uplifted region of folded and faulted Mesozoic and Cenozoic sedimentary and volcanic rocks. Between 1984 and 2021, the dam experienced several earthquake events, with 16 earthquake recordings captured and archived in the CSMIP database. The accelerograms were bandpass filtered between *0.30* and *40 Hz*, and instrument- and baseline-corrected by the CSMIP. Fig. 5 shows the names, dates, and epicenters of these events in relation to the dam's location, while Table 2 provides a summary of the earthquake records, including their names, dates, and record sequence numbers (RSNs).

Electronic supplement-A provides a detailed summary of the *16* seismic events recorded at Briones Dam, including key parameters such as magnitude (M_w), epicentral distance (R_{Epi}), hypocentral distance (R_{Hyp}), peak horizontal accelerations (PGA_{tran} and PGA_{long}) vertical accelerations (PGA_{up}), Arias intensity (I_a),and cumulative absolute velocity (CAV) for transverse, longitudinal, and vertical directions. The sensors at the left abutment, center, and left crest are designated as Loc1, Loc2, and Loc3. The earthquakes occurred at epicentral distances ranging from *6* to *35* kilometers, with magnitude (M_w) ranging between *3.3 to 6.0*. Peak ground acceleration (PGA) ranged from *0.01 g* to *0.18 g* (geometric mean of the two horizontal components). The largest PGA, *0.18g*, at the dam was recorded at the left crest during the M_w*4.2* Piedmont Earthquake on July 20, 2007, which occurred at an epicentral distance (Repi.) of *12 km*. Overall, these relatively low-intensity events (e.g. < *0.2g*, Park and Kishida (2019)) are useful for predicting the linear fundamental behavior of the dam.

Table 2. Earthquake events recorded at Briones Dam

Record Sequence Number (RSN)	Earthquake Name	Time	M_w
2	Piedmont Earthquake of 20 Dec 2006	7:12:28 PM PST	3.6
3	Piedmont Area Earthquake of 20 Jul 2007	4:42:22 AM PDT	4.2
4	South Napa Earthquake of 24 Aug 2014	03:20:44 PDT	6.0
5	Piedmont Earthquake of 17 Aug 2015	06:49:17.320 AM PDT	4.0
6	Lafayette Earthquake of 01 Mar 2007	8:40:00 PM PST	4.1
7	San Leandro Earthquake of 23 Aug 2011	11:36:54 PM PDT	3.5
8	Berkeley Earthquake of 20 Oct 2011	2:41:04 PM PDT	4.0
9	Berkeley Earthquake of 20 Oct 2011	8:16:05 PM PDT	3.8
10	Berkeley Earthquake of 27 Oct 2011	5:36:44 AM PDT	3.5
11	El Cerrito Earthquake of 05 Mar 2012	5:33:19 AM PST	3.9
12	Berkeley Earthquake of 04 Sep 2003	18:39:53 PDT	3.8
13	Berkeley Earthquake of 04 Jan 2018	02:39:37.730 PST	4.4
14	Berkeley Earthquake of 22 Dec 2006	22:49:57.00 PST	3.5
15	Berkeley Earthquake of 23 Dec 2006	9:21:15.00 PST	3.3
16	Pleasant Hill Earthquake of 14 Oct 2019	22:33:42.810 PDT	4.5
17	San Lorenzo Earthquake of 28 Jun 2021	18:29:48.060 PDT	3.9

Microtremor Measurements

Ambient noise measurements were collected on June 2, 2024, by Dr. Nweke Chukwuemeka Chukwuebuka, Dr. Athanasopoulos-Zekkos, and Dr. Makbule Ilgac, at 7 locations across the dam crest, abutment, and toe. These collection points were labeled USC 1-7, as shown in Fig. 6a. For the measurements, Nanometric 120 Second Trillium Compact symmetric triaxial-sensor seismometers were used, along with Pegasus digitizers, which were connected to each other as well as to a battery. The components for each sensor deployment are shown in Fig. 6b. Finally, at the toe location (USC-7), Table 3 provides the GPS coordinates of each sensor along with the measurement times.

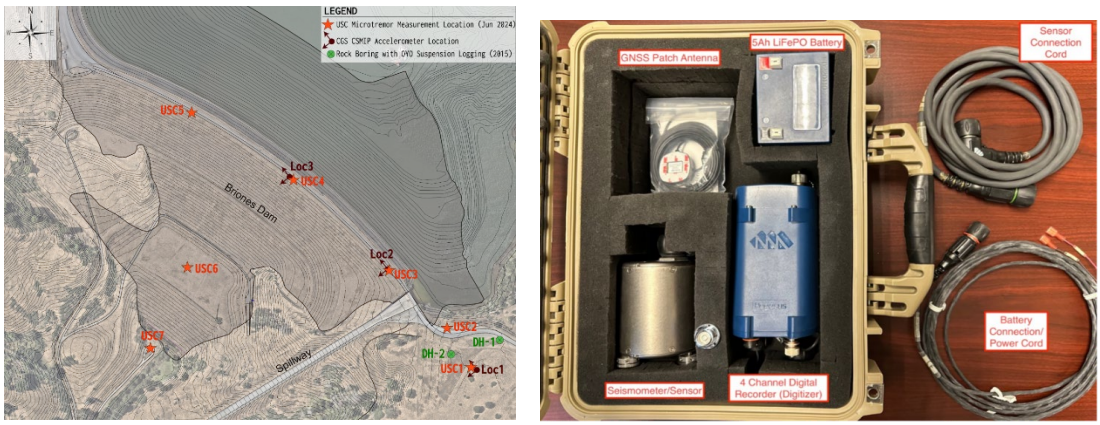

Fig. 6 (a). Location of the microtremor measurements on Briones Dam, (b) The sensor setup includes the Pegasus digitizer, connecting cords, and a battery.

Table 3. Location of microtremor measurements and recording times.

Site ID	Starting Elevation (m)	Latitude	Longitude	Start Time UTC	End Time UTC
BD-USC1	196.6	37.910610	-122.205323	8:03:53 PM	11:23:02 PM
BD-USC2	194.5	37.911188	-122.205865	7:59:34 PM	11:31:24 PM
BD-USC3	186.5	37.911997	-122.206993	8:21:51 PM	11:43:56 PM
BD-USC4	191.6	37.913282	-122.208735	8:40:05 PM	11:54:06 PM
BD-USC5	192.6	37.914198	-122.210447	8:56:06 PM	12:03:11 AM
BD-USC6	132.1	37.911954	-122.210576	9:32:01 PM	12:28:23 AM
BD-USC7	106.4	37.910830	-122.211208	9:53:26 PM	12:37:41 AM

Vibration Characteristics of Briones Dam

The vibration characteristics of Briones Dam were assessed using earthquake recordings available in the CMSIP database, and ambient noise measurements collected at various locations on the dam. The analyses using earthquake recordings that provide the eHVSR and SSR at the center and left crest have been presented in previous publications (Ilgac and Athanasopoulos-Zekkos, 2023) and will not be repeated herein. The paper will focus on the microtremor measurements and subsequent analyses to assess mHVSR. mHVSR is calculated at the abutment, crest, mid-dam, and toe locations.

Microtremor-based Horizontal to Vertical Ratio (mHVSR)

Microtremor measurements are gathered using triaxial seismic sensors. The noise recordings are divided into time windows of a certain length, each of which is Fourier transformed and then smoothened using the Konno–Ohmachi window method (Konno and Ohmachi, 1998) with a smoothing coefficient "*b*" set to value of 40. Microtremor-based HVSR (mHVSR) is then calculated by dividing the geometric mean of the two horizontal components by its vertical component. The median and standard deviation of mHVSR are calculated, either arithmetically or logarithmically to produce an mHVSR curve. Resonant peaks (f_s) are selected from the mean curve as one indication/determination of the site's vibration characteristics. mHVSR has been proven to be a reliable tool for site characterization and for calculation of the fundamental frequency (or period) of the site, as supported by numerous studies (e.g., Konno and Ohmachi (1998), Bonnefoy-Claudet et al. (2008), Yong et al. (2013), Hassani and Atkinson (2019), Cox et al. (2020), Molnar et al. (2022), and others).

For Briones Dam, the ambient noise measurements collected at the seven locations (USC1-7) are processed using the *hvsrpy* code (Vantassel, 2020; Cox et al., 2020; Cheng et al., 2020). This code enables an automated processing of microtremors that adheres to the standards detailed above (dividing the measurement into time windows, applying cosine tapering, Fourier transforms, and smooths using the Konno and Ohmachi (1998) function, where the input parameters). The algorithm is also capable of window rejection, where the fundamental frequency of each individual mHVSR curve is statistically evaluated, and the outliers are

removed if they exceed a specific standard deviation. Once complete with the window rejection, the logarithmic median curve is recomputed, and an updated fundamental frequency of the site (f_{0mc}) is determined. Alternatively, the logarithmic mean (μ_{lnf0}) and standard deviation (σ_{lnf0}) using the individual time windows ($f_{0,i}$) are also calculated, allowing for a statistical evaluation of the fundamental frequency of the site of interest. In addition, *hvsrpy* screens the mHVSR results based on the reliability and clearness criteria prescribed by SESAME (2004). The details regarding the algorithm can be found in Vantassel (2020) and Cox et al. (2020).

The SESAME (2004) guidelines provide a well-established criteria for processing microtremor data, including three reliability checks (to assess the reliability of the mHVSR curve) and six clearness criteria (to determine if the fundamental frequency is clearly identified). The site's fundamental frequency is considered valid if it satisfies all reliability checks and at least five of the six clearness criteria. According to these guidelines, many windows are required, and the total number of significant cycles (n_c) should exceed *200*. The significant number of cycles is calculated as a function of the fundamental frequency of the site of interest as $n_c=I_w.n_w.f$, where I_w is the window length, n_w is the number of windows, and f is the fundamental frequency. In our analysis at seven locations on Briones Dam, records of at least 20 minutes were used, with multiple 60-minute recordings also available. A window length of 60 seconds was chosen, with 5% cosine tapering applied at both ends, and a Konno and Ohmachi (1998) smoothing bandwidth "*b*" of 40. As noted in the SESAME guidelines, caution is advised when conducting measurements near structures, as wind-induced movements of nearby buildings or trees can cause low-frequency noise. This was carefully considered when interpreting the mHVSR results. Additionally, as discussed by Cheng et al. (2020), variability in fundamental frequency can arise from HVSR analysis when the assumptions of an azimuthally isotropic noise wavefield, a flat 1-D site, and homogeneous horizontally stratified subsurface layers do not hold. Given that Briones Dam is a 3D structure in a valley, topographical influences were expected, and azimuthal variability was computed accordingly.

Fig. 7 shows the field condition at Briones Dam during the collection of ambient noise measurements, with Fig. 7a showing the left abutment sensor (USC1), which is collocated with a CSMIP strong motion station (Loc 1 in Figures 1 & 6) that provided earthquake recordings used to estimate eHVSR. The left abutment sensor (USC1) and the strong ground motion station (Loc 1) are positioned on a hill with a *2-meter* elevation difference over a *17-meter* length, resulting in a *6-7 %* slope. This topographical feature is expected to influence/affect both mHVSR and eHVSR results. Since earthquake recordings from this site are used in SSR calculation, it is important to acknowledge the effect of topographical influence on the collected earthquake and microtremor data collected at this location. Other sensors, such as those on the crest and mid-dam, are also influenced by topographical effects. The microtremor data, initially oriented north and east, were rotated to align with the transverse (*38°*) and longitudinal (*128°*) directions of the center crest sensor. Figures 8 and 9 display the mHVSR results obtained using *hvsrpy* code for the transverse and longitudinal directions at seven locations on Briones Dam. Sensors USC-1, USC-3, and USC-4 are co-located with strong motion sensors at the left abutment, left crest, and center crest, respectively. Multiple measurements were taken at each sensor on the same day, with minimum durations and recording times listed in Table 4. In Figures 8 and 9 the triangles indicate the peaks that meet reliability criteria (blue triangles) and clearness criteria (purple triangles). Although SESAME (2004) recommends satisfying at least 5 out of 6 clearness

criteria, we also evaluated some of the fundamental frequencies that met a minimum 4 out of 6 clearance criteria (violet triangle).

In the transverse and longitudinal directions (Figures 8 & 9), all sensors displayed a low-frequency peak around *0.15 Hz*, which could be attributed to wave action in the reservoir. Although we attempted to minimize wind effects by covering the sensors with buckets, wind can still cause significant low-frequency ground disturbances (i.e., f < 1 Hz; SESAME, 2004), and this may not have been fully mitigated. Another possible cause for this low frequency could be the deep bedrock impedance ratio. However, this low-frequency value, observed at all stations, can be assumed to be unrelated to the structural characteristics (fundamental frequency) of the dam. Further investigation, such as deep shear wave velocity profiling, may help clarify whether these peaks are due to the reservoir, wind, or bedrock contrasts. For our analysis, peak selection focused on the *0.3-25 Hz* range.

Fig. 8 shows mHVSR results in transverse (upstream-downstream) direction at the seven Briones Dam locations (USC 1-7). At the left abutment (USC-1 and USC-2), no significant peaks were observed, indicating rock-like conditions. This location is founded on claystone, sandstone, and conglomerate layers having an average $V_{S30} \simeq 600$ *m/s*, representing soft rock conditions. The derived mHVSR curves at the left crest sensor (USC-3), positioned near the abutments and on a shallow part of the dam, produced an estimated fundamental frequency (f_0) of *1.4 Hz ± 0.1*, and *1.4 Hz ± 0.2* in two different segments of the ambient noise recordings (i.e., the 2nd hour and the 3rd hour), both of which satisfied reliability and clearness criteria. At the center crest location (USC-4), the fundamental frequency was estimated as *0.7 Hz ± 0.2* for one recording segment, and *0.8 Hz ± 0.3* for the subsequent recording segment, though only 4 out of 6 clearness criteria were met. At the right crest sensor (USC-5), two impedance contrasts were observed: the first frequency peak was around *1.5 Hz*, which met all the criteria, while a second peak at 8-9 Hz was also noted. The distance between the right crest sensor and the abutment was larger than on the left side, and the location of USC-6 on the mid-dam axis platforms (see Fig. 6) may have contributed to the secondary peaks. At the mid-dam location (USC-6), the secondary peak around *8-9 Hz* observed at USC-5 was detected again but it did not satisfy the SESAME (2004) reliability criteria. Finally, at the toe location (USC-7), the mHVSR curves showed no clear peaks in the transverse direction. The algorithm detected a peak at *1.7 Hz* (visually examining not a clear peak) at USC-7 in the transverse direction, which satisfies 4 out of the 6 criteria, with an amplitude ranging between *3.6* and *3.9*, while the fundamental frequency amplitude at USC-4 was much higher, between *19* and *25* at *0.7-1 Hz*.

Fig. 9 shows mHVSR results in longitudinal (cross-canyon) direction at the seven Briones Dam locations (USC 1-7). Fundamental frequencies (peaks in the mHVSR curves) around *1.4-1.5 Hz* with amplitudes between *5* and *6.5* were observed at the left abutment (USC-1) and toe (USC-7) sensors. However, only one recording segment at USC-1 satisfied the criteria checks, while the remaining measurements at the sensor did not show clear peaks. At the left crest (USC-3), peaks were detected around *1-1.4 Hz*, with amplitudes ranging from *8.5* to *14*, but only 4 out of 6 clearness criteria were satisfied. The center crest (USC-4) showed a peak at *0.7-1 Hz*, with amplitudes of *15-15.5*. The first segment of ambient noise recording at USC-4 satisfied all the criteria, while the second segment satisfied 4 out of 6 clearness criteria. Similar to the transverse direction, the right crest sensor (USC-5) showed two peaks at 1.*4* and *12 Hz*, which

indicates two impedance contrasts in the subsurface materials. The recordings from the mid-dam sensor (USC-6) showed no clear peaks, though visual examination identified peaks at 1.4-1.6 Hz and 12 Hz, consistent with the transverse direction. By examining the results at the reference sites (left abutment and toe), we observe either flat mHVSR curves, indicating rock conditions, or peaks around *1.1-1.4 Hz* at the abutment and *1.7 Hz* at the toe, with amplitudes between *2* and *6*. These peaks suggest an impedance contrast (a significant increase in Vs) at a bedrock depth of *200-400 meters*. Similar peaks were observed at the left abutment (USC-3), with a peak at *1.4 Hz* and an amplitude of 7-14. Sensors near the right abutment (USC-5) showed peaks at *1.4-1.6* and *8-9 Hz*, with an amplitude of *4-5*, which can also be attributed to the deep bedrock impedance contrast observed at abutment and toe. At the center crest, peaks shifted to *0.7-0.8 Hz* with higher amplitudes of *15-25*, likely due to the presence of the dam. However, when focused on the longitudinal direction, the relatively lower amplitude peaks at *1.4-1.7 Hz* observed at the reference sites (toe and abutment), suggest a possible connection that requires further analysis to validate the significant impedance contrast in the underlying rock layers. Therefore, we recommend conducting deep shear wave velocity measurements around Briones Dam to better visualize and understand the underlying rock conditions and further evaluate the mHVSR results.

It is important to recognize that conducting ambient noise measurements on a 3D structure like a dam is challenging. However, the distinct shift in frequency from *1.1-1.7 Hz* at the reference sites to *0.7-1 Hz* at the center crest, along with the significantly larger amplitude (2-9 times greater in the longitudinal direction and *5-14* times greater in transverse direction), can be attributed to presence of the dam. While the flat mHVSR results at the reference sites in the transverse direction indicate rock-like conditions. Overall, the results derived from microtremor measurements in the transverse direction appear more coherent, with field measurements identifying the fundamental frequency of the Briones Dam to fall between *0.7-1 Hz*.

Fig. 7. Ambient Noise measurements: a) site conditions at USC-1 where a post-hole digger was used to excavate about 12-18 inches, b) an example of the test set-up (USC-3, c) site condition at USC4, d) site condition at USC-7.

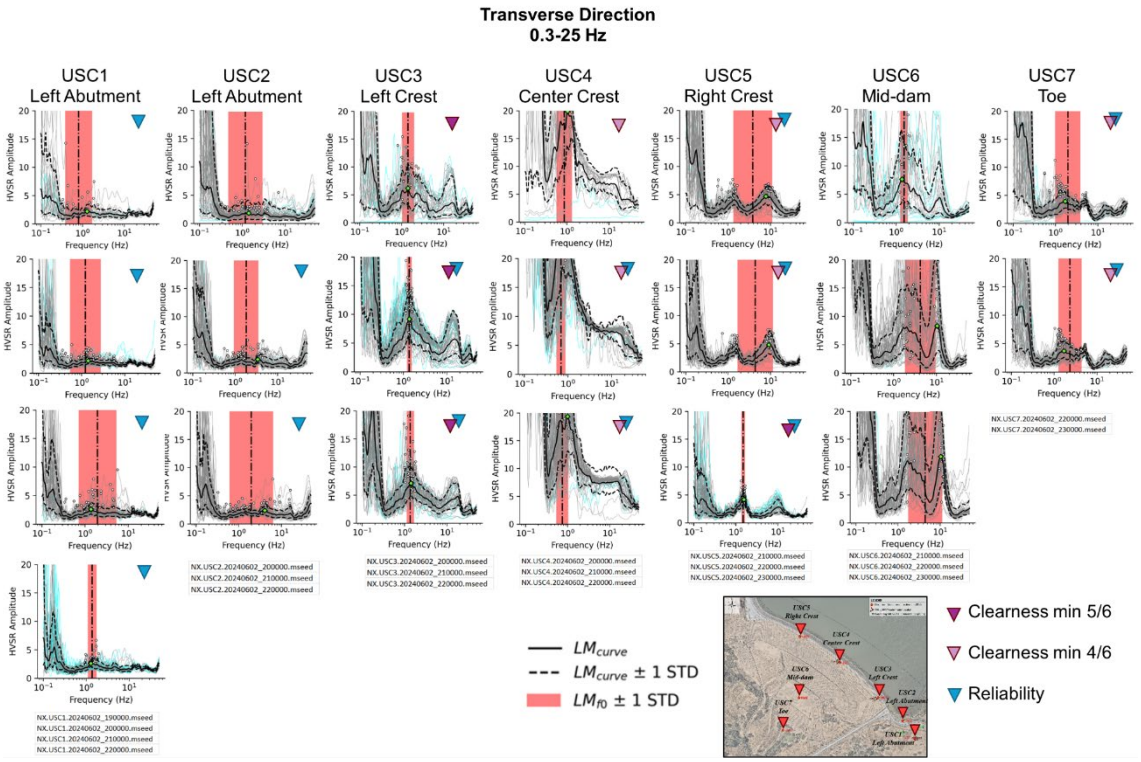

Fig. 8. mHVSR results at Briones Dam in the transverse direction. (mHVSR figures are prepared using *hvsrpy* code)

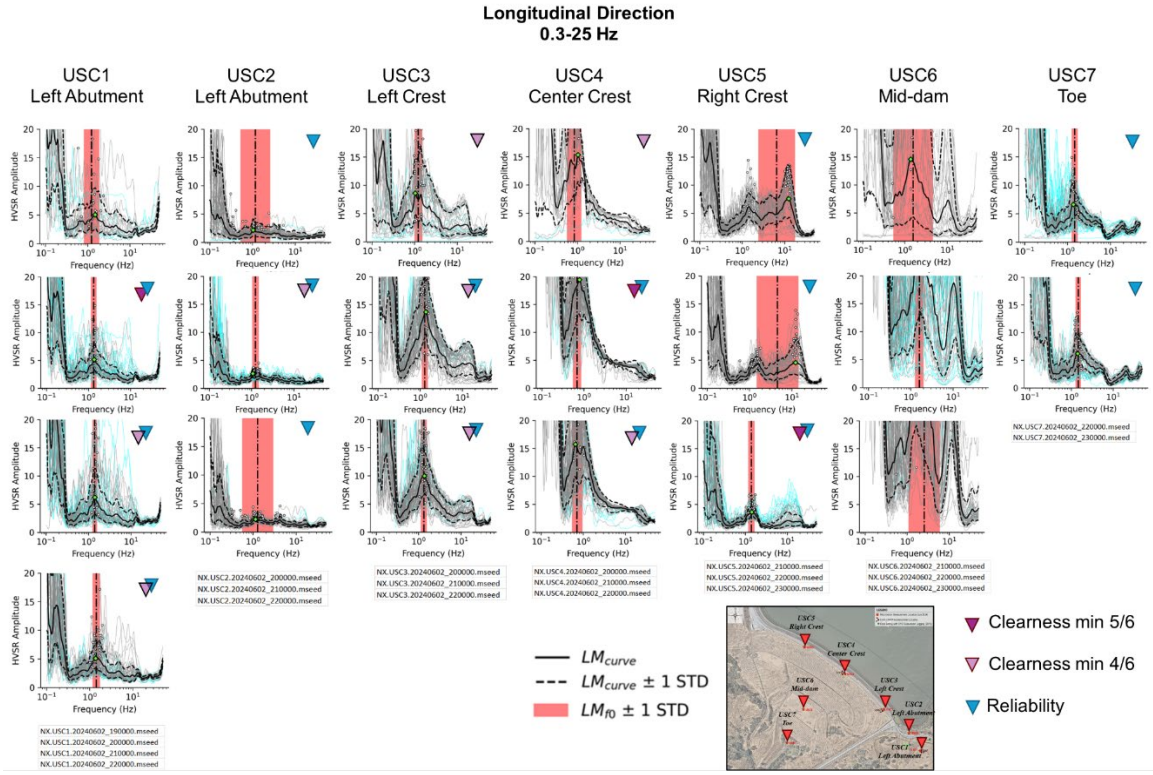

Fig. 9. mHVSR results at Briones Dam in the longitudinal direction.

Interpretation of Results

Table 4 presents the fundamental frequency values for Briones Dam, derived from measurements at the center and left crest locations in both transverse and longitudinal directions. Due to the proximity of the left crest sensor to the abutments and its placement on a shallower part of the dam, the associated results showed considerable variation across different methods and likely do not accurately reflect the dam's vibration characteristics. In contrast, the center crest sensor, located at the mid-dam span, provides a more representative description of the dam's seismic response. At the center crest in the transverse direction, the fundamental frequency from the median curve (f_{0mc}) was *0.9 Hz* based on both eHVSR and mHVSR (averaged from multiple recordings), while SSR resulted in a value of *1.2 Hz*. In the longitudinal direction, eHVSR showed a peak at *1.1-1.4 Hz*, mHVSR indicated a fundamental frequency of *0.7 Hz*, and SSR again resulted in a value of *1.2 Hz*.

Table 4. Fundamental mode frequency values (f_{0mc}) were obtained by different methods in Briones Dam at the center crest, left crest, and abutment.

		Fundamental Frequency, f_{0mc} (Hz)		
Method	**Direction**	**Center Crest (Loc2)**	**Left Crest (Loc3)**	**Left Abutment (Loc1)**
eHVSR	Longitudinal	1.1-1.4 (secondary)	1.0	First peak 0.5 second peak at 1.0
	Transverse	0.9	0.9	0.9
mHVSR	Longitudinal	0.7-0.8	1.4	1.4
	Transverse	0.8-1.0	1.4	No peak
Crest to Abutment ratio (SSR)	Longitudinal	1.2	3.1	NAP
	Transverse	1.2	2.4	NAP

The impact of azimuthal variability was also analyzed, and the results indicate that at the center crest, the fundamental frequency remains around *1 Hz* across different angles. This frequency is accompanied by a large amplitude of approximately *15*, which is attributed to the dam's structural response. As previously discussed, eHVSR was calculated using the S-wave portion of the records, with results presented in Ilgac et al (2024). At the center crest, the value of "f_o", when selected from the median curve, was *0.9 Hz* in the transverse direction and *1.1-1.4 Hz* in the longitudinal direction, consistent with values obtained when eHVSR is calculated using the full record. A comparison of both eHVSR estimates is shown in Figure 8, and further details can be found in Ilgac et al (2024). As discussed before, assessing individual earthquakes (or time windows in microtremors) enables the calculation of median and standard deviation of the fundamental frequency, assuming a lognormal distribution from individual time windows as proposed by Cox et al. (2020). Among different methods, the standard deviation of the fundamental mode frequency is found to be minimal when the SSR method is used (e.g., 0.1) and varies between 0.2 and 0.25 when eHVSR and mHVSR are implemented.

The median fundamental frequency of the dam is estimated to be approximately *1 Hz* with a maximum logarithmic standard deviation of *0.3* across different methods at the center of the dam crest. The slight variations among these three methods suggest the need for further

investigations that consider the geological and geotechnical conditions of the dam.

The reference sensor at the left abutment, positioned on sloping terrain, may not accurately reflect the bedrock conditions for Briones Dam. A more suitable reference site could be USC-2, where the flat mHVSR curves indicate bedrock-like conditions with less topographical influence. This discrepancy between the two left abutment results reveals a potential opportunity to install a vertical array of accelerometers/seismometers to monitor and record surface, bedrock, and within motions at Briones Dam, which could mitigate the influence of topography and emphasize the effect of geotechnical conditions.

The relatively subtle peak observed at the left abutment, ranging from *0.9-1.4 Hz* in the longitudinal direction (and flat in the transverse direction), suggests the need for further investigation into whether these peaks are associated with a sharp shear wave velocity (V_S) change at bedrock depths of around *100 meters*. Given the geological setting around Briones Dam, which consists of soft rock ($V_{S30} = 600$ *m/s*) and potential basin effects (due to the contrast of the soft rocks with deeper, stronger lithified rocks from the great valley sequence (Brocher, 2008)), it is likely that the small amplitude peaks observed at reference sites (toe, abutment) around *1.1-1.4 Hz* are related to the geological conditions at and around the dam. However, at the center crest, the peak frequency shifted closer to *1 Hz*, with higher amplitude and clarity. Thus, the fundamental frequency of Briones Dam is estimated to be between *0.7* and *1 Hz* (mHVSR), *0.9* and *1.1 Hz* (eHVSR), and *1.2 Hz* (SSR), with the median fundamental frequency around *1 Hz* and a maximum logarithmic standard deviation of *0.3* among different methods at the center crest. To further validate these results and gain a better understanding of the material properties, deep shear wave velocity measurements should be conducted at the bedrock and within the embankment materials. Currently, the absence of shear wave velocity data for the dam (i.e., obtained at the crest) prevents direct comparison of Briones Dam's fundamental frequency with analytical models from the literature.

Conclusions

The vibration characteristics of dams have been studied extensively through case histories, and the use of analytical models such as the shear beam approach, which establishes correlations between dam period, shear wave velocity (V_S), and dam geometry. However, at Briones Dam, V_S measurements for the dam material are unavailable, making direct comparisons with analytical solutions impossible. While systematic evaluations of dam fundamental frequencies using ground motion data have been conducted in Japan, such as studies examining the effects of peak acceleration (a_{max}) and dam height on the fundamental period (e.g., Park and Kishida 2019), comprehensive assessments that integrate field measurements with empirical approaches remain limited to individuals case histories. Expanding this research is essential for improving our understanding of dam behavior and refining predictive models. The availability of the earthquake recordings at Briones Dam provides an opportunity to assess its dynamic characteristics. Several methods (eHVSR, mHVSR, and SSR) were used to determine the dam's fundamental frequency yielding promising results for evaluating the dynamic behavior of dams through relatively simple approaches. The left crest sensor, located near the abutments and on a shallower section of the dam, exhibited greater variability in results, making it less representative, nor reliable for estimating the dam's overall response. In contrast, the center crest sensor, situated at the mid-dam span, proved more reliable in adequately describing/representing

the dam's seismic behavior. In the transverse direction at the center crest, the fundamental frequency from the median curve was estimated to be *0.9 Hz* using eHVSR and mHVSR (averaged from multiple recordings), while SSR yielded a frequency of *1.2 Hz*. In the longitudinal direction, eHVSR indicated a fundamental frequency in the range of *1.1-1.4 Hz* with an average of *1.25 Hz*, while mHVSR produced a peak at *0.7-0.8 Hz*, and SSR gave a value of *1.2 Hz*. Considering that the reference site (left abutment) is located on a sloping terrain, it may not accurately represent the bedrock conditions for Briones Dam. A more suitable reference site could be USC-2, which showed flat mHVSR curves indicative of bedrock-like conditions with minimal topographic influence. The relatively subtle peaks observed at the left abutment in the longitudinal direction, estimated to be around *0.9-1.4 Hz*, should be further investigated to determine if they are related to a deep bedrock shear wave velocity (V_S) change at approximately *100 meters*. Notably, the reference sites in the transverse direction produced flat mHVSR curves, further confirming rock-like conditions. Given the geological setting around Briones Dam, characterized as soft rock ($V_{S30} = 600$ *m/s*), and the associated potential basin effects due to deeper, stronger impedance contrasts in the area, the peak frequencies observed at *0.9-1.4 Hz* which are close to the dam's fundamental frequency of *0.7-1.2 Hz* might be influenced by these factors. To validate these findings, deep shear wave velocity measurements at the bedrock and a detailed characterization of the embankment materials are recommended. It should be acknowledged that ambient noise measurements on 3D structures like dams are challenging. However, the distinct shift in frequency values (from *1.1-1.7 Hz* to *0.7-1.2Hz*) and the significant increase in amplitude (*2-9* times larger relative to reference sites in longitudinal, and *5-14* times larger in transverse direction) observed at the center crest sensor are likely due to the dam's unique vibration characteristics.

Acknowledgments

The authors are grateful to the California Strong Motion Instrumentation Program for supporting this work. The authors are also grateful to colleagues Dr. Nweke for his help in collecting the field microtremor data, Dr. Kayen and Dr. Ktenidou for their insights in interpreting the data and to Mr. Peterson of EBMUD for securing site access and providing data on the Briones Dam.

References

Abdel-Ghaffar, A. M., & Koh, A. S. (1981). Longitudinal vibration of non-homogeneous earth dams. Earthquake Engineering & Structural Dynamics, 9(3), 279-305.

Abdel-Ghaffar, A. M., & Scott, R. F. (1979a). Analysis of earth dam response to earthquakes. Journal of the Geotechnical Engineering Division, 105(12), 1379-1404.

Abdel-Ghaffar, A. M., & Scott, R. F. (1979b). Shear moduli and damping factors of earth dam. Journal of the Geotechnical Engineering Division, 105(12), 1405-1426.

Ambraseys, N. N. (1960), The seismic stability of earth dams, in `Proceedings of the 2nd World Conference on Earthquake Engineering, Tokyo.

Athanasopoulos-Zekkos, A., & Ilgac, M. (2024). Using CSMIP data to derive reliable dynamic response parameters for earth dams in California (Research Project Final Report, approved).

Bard, P. (2004). Guidelines for the implementation of the H/V spectral ratio technique on ambient vibrations: Measurements, processing, and interpretation, SESAME European Research Project, WP12—Deliverable D23, 12, EVG1-CT-2000-00026, 1–62.

Bonilla, L. F., J. H. Steidl, G. T. Lindley, A. G. Tumarkin, & R. J. Archuleta (1997). Site amplification in

the San Fernando Valley, California: Variability of site-effect estimation using the S-wave, coda, and H/V methods, Bull. Seismol. Soc. Am. 87, 710–730.

Bonnefoy-Claudet, S., Kohler, A., Cornou, C., Wathelet, M., & Bard, P.-Y. (2008). Effects of Love Waves on Microtremor H/V Ratio. Bull. Seismol. Soc. Am. 98, 288–300. https://doi.org/10.1785/0120070063

Borcherdt, R. D. (1970). Effects of local geology on ground motion near San Francisco Bay. Bulletin of the Seismological Society of America, 60(1), 29-61.

Boulanger, R. W., Bray, J. D., Merry, S. M., & Mejia, L. H. (1995). Three-dimensional dynamic response analyses of Cogswell Dam. Canadian geotechnical journal, 32(3), 452-464.

Brocher, T. M. (2008). Compressional and shear-wave velocity versus depth relations for common rock types in northern California. Bulletin of the Seismological Society of America, 98(2), 950-968.

California Department of Water Resources. Retrieved 2023, from http://cdec.water.ca.gov/

California Geological Survey and U.S. Geological Survey (2005). Center for Engineering Strong Motion Data (CESMD). U.S. Geological Survey https://doi.org/10.5066/P13HTZQS

Can, G., Askan, A., & Karimzadeh, S. (2021). An assessment of the 3 February 2002 Cay (Turkey) earthquake (Mw= 6.6): Modeling of ground motions and felt intensity distribution. Soil Dynamics and Earthquake Engineering, 150, 106832.

Cetin, K. O., Isik, N. S., Batmaz, S., & Karabiber, S. (2005). A comparative study on the actual and estimated seismic response of Kiralkizi Dam in Turkey. Journal of earthquake engineering, 9(04), 445-460.

Cheng, T., Cox, B. R., Vantassel, J. P., & Manuel, L. (2020). A statistical approach to account for azimuthal variability in single-station HVSR measurements. Geophysical Journal International, 223(2), 1040-1053.

Correia, N., & Pasten, C. (2019). Using Seismic Records to Determine the Predominant Vibration Frequency of a Tailings Dam Embankment: First Results. In 6th International Seminar on Tailings Management, Tailings.

Cox, B.R., Cheng, T., Vantassel, J.P., & Manuel, L., (2020). A statistical representation and frequency-domain window-rejection algorithm for single-station HVSR measurements. Geophys. J. Int. 221, 2170–2183. https://doi.org/10.1093/gji/ggaa119

Di Giacomo, D., Gallipoli, M. R., Mucciarelli, M., Parolai, S., & Richwalski, S. M. (2005). Analysis and modeling of HVSR in the presence of a velocity inversion: the case of Venosa, Italy. Bulletin of the Seismological Society of America, 95(6), 2364-2372.

East Bay Municipal Utility District. (1967). Briones Project Report.

Field, E.H., & Jacob, K.H., (1995). A Comparison and Test of Various Site-Response Estimation Techniques, including Three That Are Not Reference-Site Dependent. Bull. Seismol. Soc. Am. 85, 1127–1143.

Gazetas, G. (1987). Seismic response of earth dams: some recent developments. Soil dynamics and earthquake engineering, 6(1), 2-47.

Ghofrani, H., G. M. Atkinson, & K. Goda (2013). Implications of the 2011 M 9.0 Tohoku Japan earthquake for the treatment of site effects in large earthquakes, Bull. Earthq. Eng. 11, 171–203.

Haghshenas, E., P. Y. Bard, N. Theodulidis, & SESAME WP04 Team (2008). Empirical evaluation of microtremor H/V spectral ratio, Bull. Earthq. Eng. 6, 75–108.

Haryanto, W., Prasetio, A., Mulyo, A., & Zakaria, Z. (2018). Seismicity of Batubesi Dam at Sorowako Region Based on Earthquake Data and Microtremor Measurement. International Journal of Engineering, 31(8), 1180-1186.

Hassani, B., Yong, A., Atkinson, G. M., Feng, T., & Meng, L. (2019). Comparison of site dominant frequency from earthquake and microseismic data in California. Bulletin of the Seismological Society of America, 109(3), 1034-1040.

Hassani, B., & G. M. Atkinson (2018). Application of a site-effects model based on peak frequency and average shear-wave velocity to California, Bull. Seismol. Soc. Am. 108, 351–357.

Hassani, B., &Atkinson, G.M., (2016). Applicability of the Site Fundamental Frequency as a VS 30

Proxy for Central and Eastern North America. Bull. Seismol. Soc. Am. 106, 653–664. https://doi.org/10.1785/0120150259

Hwang, J. H., Wu, C. P., & Chou, J. T. (2008). Motion characteristics of compacted earth dams under small earthquake excitations in Taiwan. In Geotechnical Earthquake Engineering and Soil Dynamics IV (pp. 1-12).

Ilgac, M., & Athanasopoulos-Zekkos, A. (2022). Using CSMIP data to derive reliable values of dynamic response parameters for earth dams in California. In Proceedings of the SMIP22 (Strong Motion Instrumentation Program) Seminar on Utilization of Strong-Motion Data.

Ilgac, M., & Athanasopoulos-Zekkos, A. (2023). Assessment of vibration characteristics of Briones and Terminus Dams using earthquake recordings. In Proceedings of the SMIP23 (Strong Motion Instrumentation Program) Seminar on Utilization of Strong-Motion Data.

Ilgac, M., Athanasopoulos-Zekkos, A., & Ktenidou, O. (2024). Estimation of dam vibration characteristics from ground motion records– An illustrative example: Briones Dam, California. In Proceedings of the 8th International Conference on Earthquake Geotechnical Engineering (8 ICEGE), Osaka, Japan.

Kawase, H., Sanchez-Sesma, F.J., & Matsushima, S., (2011). The Optimal Use of Horizontal-to-Vertical Spectral Ratios of Earthquake Motions for Velocity Inversions Based on Diffuse-Field Theory for Plane Waves. Bull. Seismol. Soc. Am. 101, 2001–2014. https://doi.org/10.1785/0120100263

Kishida, T., Ktenidou, O. J., Darragh, R. B., & Walter, S. (2016). Semi-automated procedure for windowing time series and computing Fourier amplitude spectra (FAS) for the NGA-West2 database.

Konno, K., & Ohmachi, T. (1998). Ground-motion characteristics estimated from spectral ratio between horizontal and vertical components of microtremor. Bulletin of the Seismological Society of America, 88(1), 228-241.

Ktenidou O.-J., F.J. Chávez-García, & K. Pitilakis (2011). 'Variance reduction and signal-to-noise ratio: reducing uncertainty in spectral ratios'. Bull. Seismol. Soc. Am. 101(2), pp. 619–634. (https://doi.org/10.1785/0120100036)

Ktenidou, O. J., Chávez-García, F. J., Raptakis, D., & Pitilakis, K. D. (2016). Directional dependence of site effects observed near a basin edge at Aegion, Greece. Bulletin of Earthquake Engineering, 14, 623-645.

Kwak, D. Y., J. P. Stewart, S. U. J. Mandokhail, & D. Park (2017). Supplementing VS30 with H/V spectral ratios for predicting site effects, Bull. Seismol. Soc. Am. 107, 2028–2042.

Kawase, H., Nagashima, F., Nakano, K., & Mori, Y. (2019). Direct evaluation of S-wave amplification factors from microtremor H/V ratios: Double empirical corrections to "Nakamura" method. Soil Dynamics and Earthquake Engineering, 126, 105067.

Lachet, C., D. Hatzfeld, P. Y. Bard, N. Theodulidis, C. Papaioannou, & A. Savvaidis (1996). Site effects and microzonation in the city of Thessaloniki (Greece). Comparison of different approaches, Bull. Seismol. Soc. Am. 86, 1692–1703

Lermo, J., & Chávez-García, F.J., (1993). Site effect evaluation using spectral ratios with only one station. Bull. Seismol. Soc. Am. 83, 1574–1594.

Matsumoto, N. (2010). The recent earthquakes and dam safety in Japan. na.

Mejia, L. H., Seed, H. B., & Lysmer, J. (1982). Dynamic analysis of earth dams in three dimensions. Journal of the Geotechnical Engineering Division, 108(12), 1586-1604.

Mejia, L. & Dawson, E. (2008) Analysis of Seismic Response of Seven Oaks Dam, Data Utilization Report, CSMIP, California Dept of Conservation, Division of Mines and GeologyMakdisi et al. (1982)

Molnar, S., Sirohey, A., Assaf, J., Bard, P. Y., Castellaro, S., Cornou, C., ... & Yong, A. (2022). A review of the microtremor horizontal-to-vertical spectral ratio (MHVSR) method. Journal of Seismology, 26(4), 653-685.

Nagoshi, M., & Igarashi, T. (1971). On the amplitude characteristics of microtremors (part 2). Zisin, 45, 26-40.

Nakamura, Y. (2000). Clear identification of fundamental idea of Nakamura's technique and its applications. In Proceedings of the 12th world conference on earthquake engineering (Vol. 2656, pp. 1-8).

Nakamura, Y., (1989). A method for dynamic characteristics estimation of subsurface microtremor on the ground surface. Q. Rep. Railw. Tech. Res. Inst. 30, 25–33.

Oner, M. (1984). Estimation of the fundamental period of large earthfill and rockfill dams, Soils and Foundations 24, 1–10.

Park, D., & Kishida, T. (2019). Seismic response of embankment dams based on recorded strong-motion data in Japan. Earthquake Spectra, 35(2), 955-976.

Pastén, C., Peña, G., Comte, D., Díaz, L., Burgos, J., & Rietbrock, A. (2023). On the Use of the H/V Spectral Ratio Method to Estimate the Fundamental Frequency of Tailings Dams. Journal of Earthquake Engineering, 27(6), 1649-1664.

Pelecanos, L. (2013). Seismic response and analysis of earth dams (Doctoral dissertation, Imperial College London).

Prevost, J. H., Abdel-Ghaffar, A. M., & Lacy, S. J. (1985). Nonlinear dynamic analyses of an earth dam. Journal of Geotechnical Engineering, 111(7), 882-897.

Ruiz, E., & Pando, M. (2011). Use of Ambient Vibration Measurements to Infer Dynamic Properties of Poorly Characterized Old Earth Dams—A Case History from Puerto Rico. In Geo-Frontiers 2011: Advances in Geotechnical Engineering (pp. 1842-1851).

Sasaki, T., Ohmachi, T., & Matsumoto, N. (2018). Analysis on acceleration data of dams collected by JCOLD. In Validation of Dynamic Analyses of Dams and Their Equipment (pp. 3-30). CRC Press.

SESAME, (2004). Guidelines for the Implementation of the H/V Spectral Ratio Technique on Ambient Vibrations Measurements, Processing, and Interpretation. (No. WP12- Deliverable D23.12). European Commission - Research General Directorate.

TERRA (2016). Design of Briones Inlet/Outlet Tower Retrofits, TM-02 Results of Site-Specific VS30 Measurements

Theodulidis, N., Bard, P.-Y., Archuleta, R., & Bouchon, M., (1996). Horizontal-to-vertical spectral ratio and geological conditions: The case of Garner Valley Downhole Array in southern California. Bull. Seismol. Soc. Am. 86, 306–319.

Vantassel, J. (2020). jpvantassel/hvsrpy: latest (Concept). Zenodo. http://doi.org/10.5281/zenodo.3666956

Verret, D., LeBœuf, D., & Péloquin, É. (2021). Site effects of the Denis-Perron dam (SM-3): A case study in Eastern North America. Earthquake Spectra, 37(1_suppl), 1602-1625.

Wang, F., Tulamaiti, Y., Fang, H., Yu, X., & Zhou, C. (2023). Seismic response characteristics of polymer anti-seepage wall in earth dam based on earthquake wave motion input method. In Structures (Vol. 47, pp. 358-373). Elsevier.

Yong, A., Martin, A., Stokoe, K., & Deihl, J., (2013). ARRA-funded VS30 measurements using multi-technique approach at strong-motion stations in California and central-eastern United States (U.S. Geological Survey Open-File Report No. 2013–1102). U.S. Geologic Survey.

Zhu, C., Cotton, F., & Pilz, M. (2020). Detecting site resonant frequency using HVSR: Fourier versus response spectrum and the first versus the highest peak frequency. Bulletin of the Seismological Society of America, 110(2), 427-440.